Indian Journal of Engineering & Materials Sciences
Vol. 29, February 2022, pp. 100-107

Effects of quenching methods on shape memory properties of Cu-28Zn-3Al wt. % alloy produced by gravity casting

A Setyani[a], I A Setiawan[a], D R K Pertiwi[a] , & B T Sofyan[a,b*]

[a]Department of Metallurgy and Materials Engineering, Universitas Indonesia, Kampus UI Depok, 16424, Indonesia

[b] Faculty of Defence Technology, Indonesia Defence University, Indonesia Peace and Security Center, Sentul, Bogor 16810, Indonesia

Received: 05 February 2021; Accepted: 05 August 2021

In recent years, Cu-Zn-Al alloys are studied intensively due to their excellence in shape memory effect (SME), good mechanical properties, along with accessible production process and cost. Cu-Zn-Al Shape Memory Alloy easily form stabilization in martensite phase that leads to SME properties reduction, but can be minimized by applying alternative quenching methods. In this research, several quenching methods are proposed to minimize the phase stabilization of martensite. The Cu-28Zn-3Al alloy was produced by gravity casting and homogenized at 800 ℃ for 2h followed by air cooling. Furthermore, as-homogenized plate was betatized at 850 ℃ for 30 minutes and then subsequently quenched using three different methods: direct quench (DQ), up quench (UQ), and step quench (SQ). Morphology, phase transformation, hardness, and strain recovery characterization are examined using an optical microscope, SEM-EDS, XRD, DSC, Vickers, and bending tests. The results showed that the DQ and UQ samples consist of V-shape β'[M18R] martensite as a matrix and retained α[A1] as the second phase. The volume fraction ratio of β'[M18R]: α[A1] is (98.4:1.6) and (92.9:6.1) for DQ and UQ, respectively. However, the SQ sample did not indicate the presence of the martensite phase and did not show any recovery rate. Bending test showed that DQ and UQ had 27.2% and 36.3% of recovery rate, respectively.

Keywords: Shape memory alloy, Shape memory effect, Cu-Zn-Al, Quenching method, Martensite phase

1 Introduction

Shape Memory Alloy (SMA) is a smart material that can recover pre-deformed shape after exposure to heat at a specific temperature. Its ability to recover the initial condition is referred to as the Shape Memory effect (SME). The SMA is fabricated by forming a martensite phase from a non-diffusional transformation in which the austenite phase (parent phase) transforms into a twinned martensite phase upon rapid cooling. Twinning developed in the martensite then accommodate SME by complex movements of atoms[1]. In martensite transformation, the cooling rate plays a role in determining the phase characteristics formed, which will affect the SME. The application of this material is broad, covering the fields of aerospace, automotive, biomedical, thermal, and industrial actuators[2]. Cu-Zn-Al alloys were currently chosen to be developed into SMA as an alternative to Ni-Ti due to low production costs and easy manufacturing processes. Furthermore, Cu alloys have a better SME compared to Fe alloys, and they have high thermal and electrical stability[2-3].

Cu-Zn-Al alloys exhibit the properties of shape memory in a certain composition range. Martensite phase transformation in Cu-based SMA generally occurs in the β phase, which has a BCC crystal structure[4]. The β phase has an initial structure in the form of [A2], a disordered face-cantered cubic phase. When cooling, the structure undergoes nearest neighbor ordering (nn), forming a [B2] superlattice structure[4-7]. Further cooling results in further ordering, forming the [DO3] or [L21] superlattice phase depending on the chemical composition or cooling rate. Quenching with a high cooling rate causes the ordered phase formed to change into a martensite phase in the form of 18R, 9R, or 2H. The dominant phase formed is the 18R or 9R, and in alloys that have e/a ratio greater than 1.52, 2H is formed[8]. The phase transformation is summarized as follow: β [BCC]/ [A2] → [B2] → [D03]/ [L21] → [M18R]/ [M9R]/ [M2H].

In their development, Cu-Zn-Al alloys have the disadvantages of being low ductility, quickly aged at room temperatures and easy to form stable martensite which decreases SME. To accommodate SME, atoms of the alloy must have a high capability to deform by

*Corresponding author (E-mail: bondan@eng.ui.ac.id)

Table 1 — Nominal composition of the as-homogenized alloys (wt.%)

Element	Cu	Zn	Al	Fe	Pb	Mn	S	Cr	Pb	Sn	Co	Zr
% wt	Bal	28.2	2.94	<0.005	0.014	0.011	0.006	0.014	0.0013	0.052	0.02	0.002

detwinning while showing the low ability of diffusional transformation. Therefore, determining the alloy composition and optimal quenching method is crucial to get an SMA by having metastable martensite phase. Therefore, this study focuses on finding out the effects of the quenching methods (DQ, UQ, and SQ) on the shape memory properties of Cu-28Zn-3Al wt. % alloy. The selection of alloy composition with low Al is utilized to avoid brittleness and low transformation temperatures.

2 Materials and Methods

Cu-28Zn-3Al wt.% alloy was fabricated by gravity casting, using 99.5 % Cu rods from UD. Metallindo Sejahtera, 99.99 % Zn ingots from Korea Zinc Co. Ltd and Al ingots (99 %) from PT. Inalum. The alloy was melted at 1150 ± 5 ℃, followed by a pouring process into the 110 × 110 × 6 mm^3 AISI H-13 mold, which was preheated at 800 ℃. The as-cast plate was then homogenized at 850 ± 5 ℃ for 2h followed by air cooling. As-homogenized samples were characterized using optical emission spectroscopy (OES) composition analysis, and the nominal composition is shown in Table 1.

The as-homogenized plate was then cut into 3 specimens each with 50 x 20 x 6 mm^3 dimension using a band saw then betatized at 850 ℃ for 30 minutes and subsequently quenched with 3 different methods:

a) Direct quench (DQ); into water + dry ice bath (± 4 ℃) for 30 minutes.
b) Up Quench (UQ); into water + dry ice bath (± 4 ℃) for 30 minutes, followed by quenching into 100 ℃ boiling water for 30 minutes.
c) Step Quench (SQ); into boiling water at 100 ℃ for 30 minutes, followed by quenching into water + dry ice bath (± 4 ℃) for 30 minutes.

Samples that have been quenched are then stored in a freezer to avoid ageing. The characterizations of the Cu-28Zn-3Al wt. % was carried out by observing the microstructure using Zeiss Primotech Optical Microscope and Scanning Electron Microscope / Energy Dispersive Spectroscopy (SEM / EDS) JEOL JSM-6510LA. Quantitative calculation of the volume fractions of the phase was done using Image Pro analysis software. Samples were prepared through a standard grinding and polishing process followed by etching with $FeCl_3$. Characterization for phase transformation after quenching was carried out using Perkin Elmer STA 6000 DSC at a temperature range of 28–100 ^oC with a rate of 10 ^oC/min, X-Ray Diffraction (XRD) testing for phase identification, Microvickers hardness, and bending test. Bending test preparation was conducted by cutting each specimen with a dimension of 50 x 1 x 4 mm^3 using a low-speed diamond saw with a rotating speed of 300 rpm. Cutting using a low-speed diamond saw was intended to avoid excessive deformation and frictional heat. After that, each sample was bent at 180^o using a 20 mm rod[9]. The bent sample was then put in 100 ^oC boiling water for 15 minutes. Measurment of the shape memory effect was done by measuring the initial angle after bending (θ_s in Fig. 1) and the final angle after heating in 100 ^oC boiling water (θ_T in Fig. 1). The measurement was done manually by drawing it on paper and then measuring the angle by using a protractor. The schematic of the bending test is shown in Fig. 1

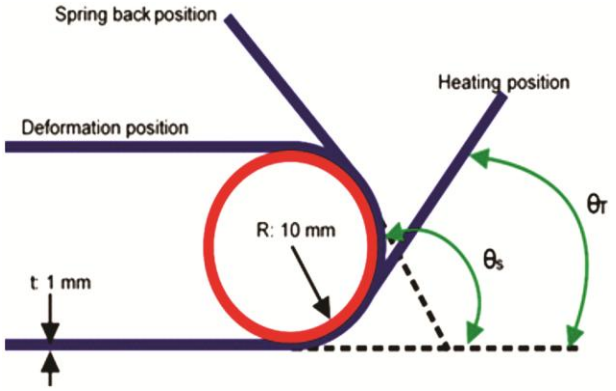

Fig. 1 — Schematic of bending test, R rods : 10 mm [9].

3 Results and Discussion

3.1 Phase Identification of as-cast and homogenized samples

Figure 2 represents the microstructures of the as-cast and as-homogenized Cu-28Zn-3Al wt. % alloys. It is clear that the microstructures of Cu-28Zn-3Al wt. % alloy consist of duplex structures (Fig. 2), they are the dark-coloured phase as matrix and the light-coloured phase as the second phase in lath morphologies. The EDS microanalysis results of the as-cast and as-homogenized samples are tabulated in Table 2. The composition of Zn and Al in spectrum 1 and 2 (second phase) contains 25.69-27.14 wt.% Zn

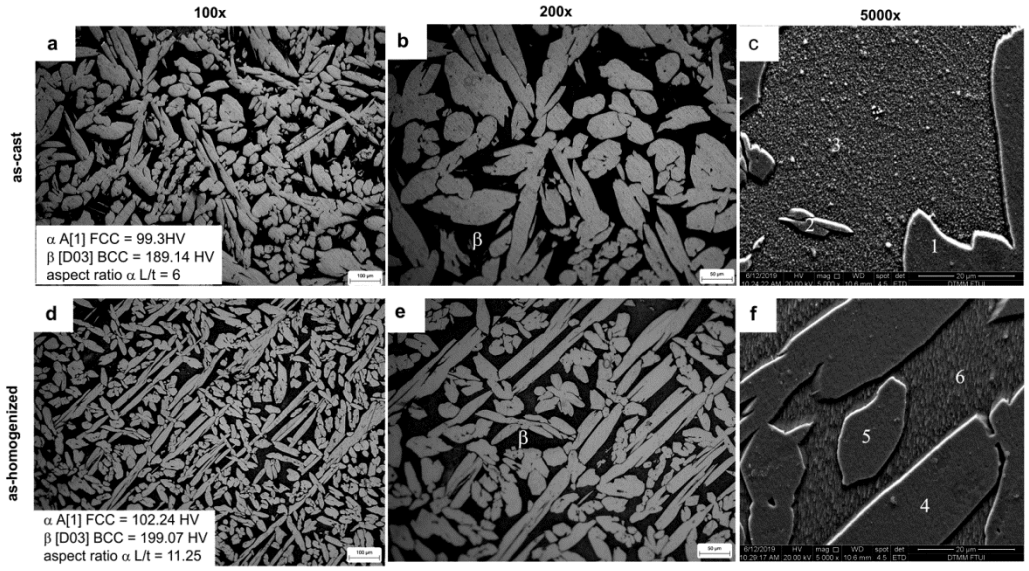

Fig. 2 — Microstructures of the (a-c) as-cast, (d-f) as-homogenized Cu-28Zn-3Al alloy. Light coloured phase in lath shape is α, and dark coloured phase is β.

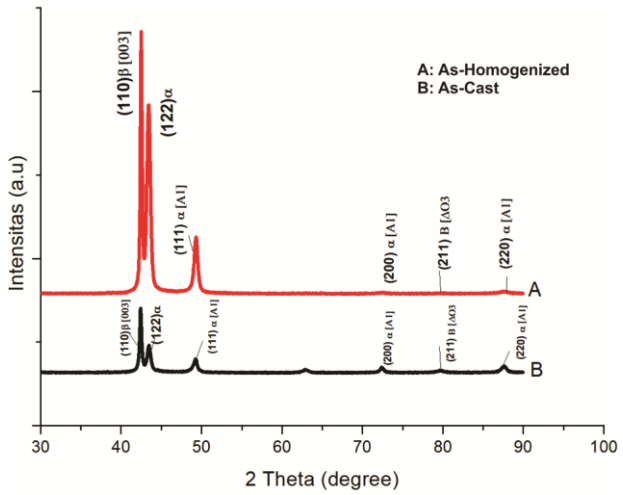

Fig. 3 — XRD diffractograms of the as-cast and as-homogenized Cu-28Zn-3Al alloy.

and 4.88 - 5.66 wt. % Al. This much lower than that of spectrum 3 (matrix), Zn: 28.85-30.4 wt. % and Al: 6.0-7.66 wt. %. The low content of Zn and Al in the second phase indicates that this is α phase with FCC crystal structure, whereas the matrix with higher Zn and Al content is β with BCC crystal structure. These results align with Stošić et al.[10], who found that as homogenized Cu-25Zn-4Al alloy had two phases, dendritic α with FCC structure distributed on the β matrix. When the alloy composition was plotted on the ternary Cu-Zn-Al equilibrium diagram by Liang et al.[11], it is clear that the Cu-28Zn-3Al alloy is in the two-phase area, α [FCC] and β [BCC].

Table 2 — EDS microanalysis on the as-cast and as-homogenized Cu-28Zn-3Al alloy at positions shown in Fig. 2 (c and f)

Samples	Spectrum	Element (wt%)			Phase
		Cu	Zn	Al	
A-Cast	1	69.42	25.69	4.88	α [FCC]/[A1]
	2	67.20	27.14	5.66	α [FCC]/[A1]
	3	63.58	30.4	6.02	β [BCC]/[$D0_3$]
As-Homogenized	1	68.89	26.12	4.99	α [FCC]/[A1]
	2	68.69	26.4	4.91	α [FCC]/[A1]
	3	63.49	28.85	7.66	β [BCC]/[$D0_3$]

Table 3 — Lattice parameters of phases in as-cast, and as-homogenized Cu-28Zn-3Al wt. % alloys

Sample	Phase	Lattice Parameter	2θ	hkl
As-Cast	β ($D0_3$)	a = 5.87 Å	42.39	110
			79.74	211
	α (A1)	a = 3.72 Å	43.46	122
			49.29	111
			75.39	200
			87.63	220
As-Homogenized	β ($D0_3$)	a = 5.87 Å	42.46	110
			76.58	211
	α (A1)	a = 3.72 Å	43.63	122
			49.08	111
			74.58.	200
			87.55	220

The XRD test results are shown in Fig. 3 and Table 3. From the XRD diffractogram, it is clear that the as-cast and as-homogenized have two phases, namely α [FCC]/ [A1] and β phases [BCC]/ [D03].

This is confirmed by the existence of the peaks of (111), (200), and (220), which indicate the presence of α [FCC] and the peaks of (110), (211), which comes from the β phases [BCC]. The results further confirm that the as-cast and as-homogenized alloy consists of two phases, namely α phase [FCC], which will be referred to as [A1], and β [BCC] phase, which will be referred to as [D03].

The results of quantitative analysis and further observations in Fig. 2 show that the α [FCC]: β [BCC] volume fraction in the as-cast and the as-homogenized condition is [64:36] and [62:38], respectively. Whereas the L/ d aspect ratio of the α phase changed from 6 in the as-cast state to 11.25 after homogenization. The result shows that the homogenization of Cu-28Zn-3Al alloys did not alter the volume fraction but changed the morphology of the second phase (α) to be longer and more ordered. The second phase which possesses lath or plate morphology tends to grow toward the tip or the thin section. The tip possesses to the incoherent interface so that it is easier to move compared to the basal plane which has coherent interface. As a result, the phase tends to be more easily elongated than thickening.

Table 4 — Microhardness of α [A1] and β [D03] phases in the as-cast and as-homogenized Cu28Zn-3Al. Wt. %

Phase	As-Cast (HVN)	As-Homogenized (HVN)
α phase	99.3	102.24
β phase	189.14	199.07

Table 4 shows the microhardness of α and β phases in both as-cast and as-homogenized conditions. It is clear that the α phase (light-coloured) had a lower hardness than the β phase (dark-coloured) in both conditions. Smirnov et al.[12] found that in the Cu-26Zn-5.27Al alloy with duplex phase (α + β), the hardness of the α phase was lower than the β phase. These results confirm that the light-coloured phase is α [A1] with the FCC structure, and dark-coloured phase is β [D03] with the BCC structure.

3.2 Effects of Quenching Method

The microstructures of Cu-28Zn-3Al alloy after quenching with three different methods (DQ, UQ, and SQ) are shown in Fig. 4 together with the EDS results

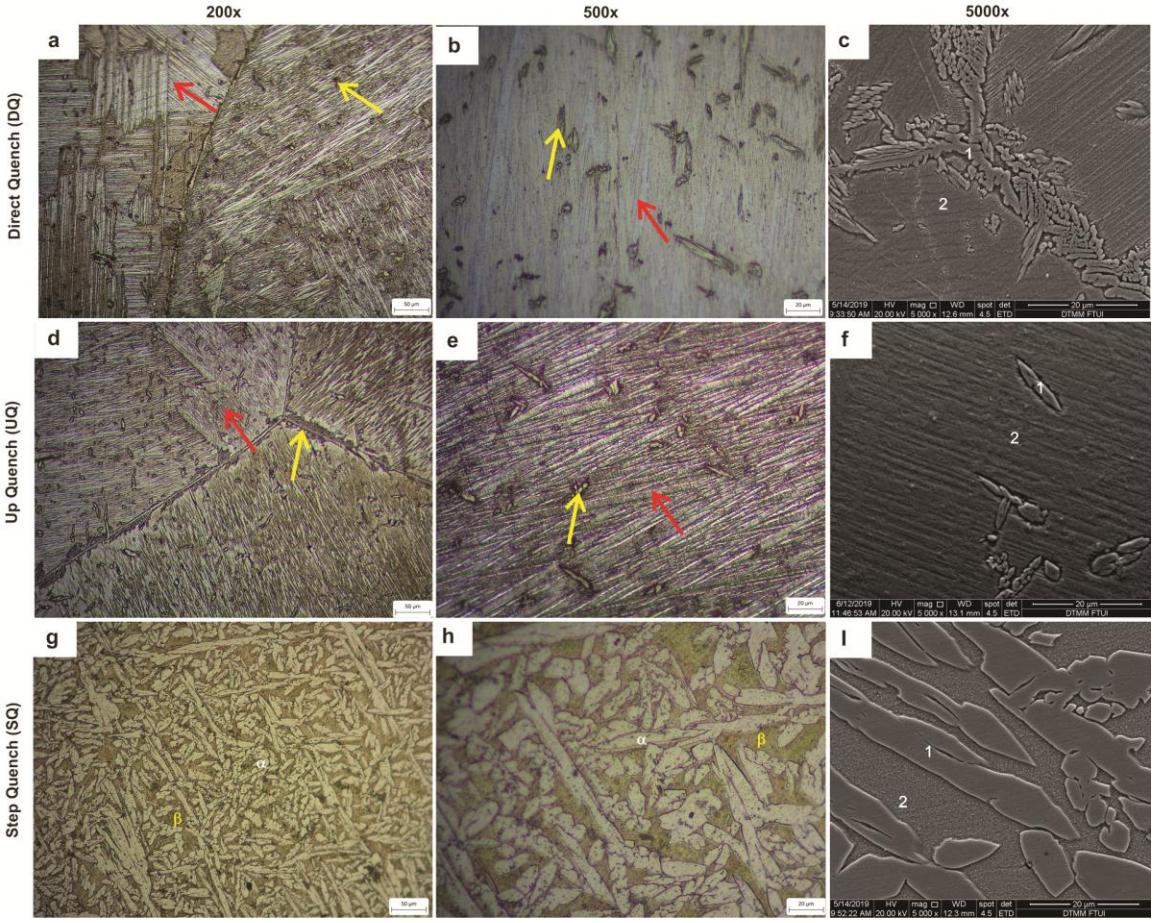

Fig. 4 — Microstructures of Cu-28Zn-3Al alloy in (a-c) DQ, (d-f) UQ, (g-i) SQ conditions. Red arrows showing the presence of β′[M18R] martensite phase in V shapes, and yellow arrows showing the presence of retained α.

in Table 5. It is seen that the DQ and UQ samples underwent phase changes, from the α [A1] + β [D03] phase in the as-homogenized condition (Fig. 2) into a phase with V-shape as the matrix (red arrows) with occurrence of small second phase distributed in the matrix (shown by yellow arrows). The V-shape phase is predicted as the martensite phase [M18R] with monoclinic structure. In contrast, the microstructures of the SQ samples resembled those of the as-cast and as-homogenized, with no V shape or needle-like phase. To further confirm identify of phase, EDS analysis was done. In the EDS results (Table 5), the Zn and Al content of the phase in position 1 in all samples is lower than that of the phase in position 2. It indicates that position 1 is α while position 2 is β. However, the morphology of the β phase in DQ and UQ samples is V-shape, indicating the β' [M18R] martensite, while the β phase in SQ sample is possibly the β [D03] phase. To further confirm the identity of the phases after quenching, samples were examined by XRD (Fig. 5), and the lattice was calculated and the results are provided in Table 6.

Table 5 — EDS microanalysis on the DQ, UQ and SQ samples of Cu-28Zn-3Al alloy at positions shown in Fig. 4 (g-i)

Sample	Spectrum	Element (wt%)			Phase
		Al	Cu	Zn	
DQ	1	3.37	70.13	26.50	α [A1]
	2	4.21	67.74	28.05	β' (martensite M18R)
UQ	1	4.35	70.18	25.47	α [A1]
	2	4.89	67.48	27.28	β' (martensite M18R)
SQ	1	2.8	71.6	25.52	α [A1]
	2	4.56	66.03	29.41	β (D03)

Figure. 5 shows the XRD diffractogram of samples in three different quenching methods. The DQ and UQ samples show peaks of (0018), (202), (208), (1210), (038), and (1418), which confirms the presence of β′[M18R] martensite phase[6]. The calculation of the lattice parameters of DQ and UQ (Table 6), confirms that the structure is monoclinic as possessed by the β′[M18R] martensite phase. The β angle and ψ tetragonality in UQ sample is higher than those of the DQ sample. Preheating at 100 ℃ in the UQ treatment gives time for the martensite to form a more perfect monoclinic crystal, so that the β angle and ψ is greater[13]. In addition to the found M18R peaks, the cubic 220 peak indicates the presence of phase α [A1], which upon calculation, the lattice parameter is found to be a = 3.62 Å, confirming the presence of α [A1] precipitates. In contrast, the XRD diffractogram of SQ indicates the presence of α [A1]

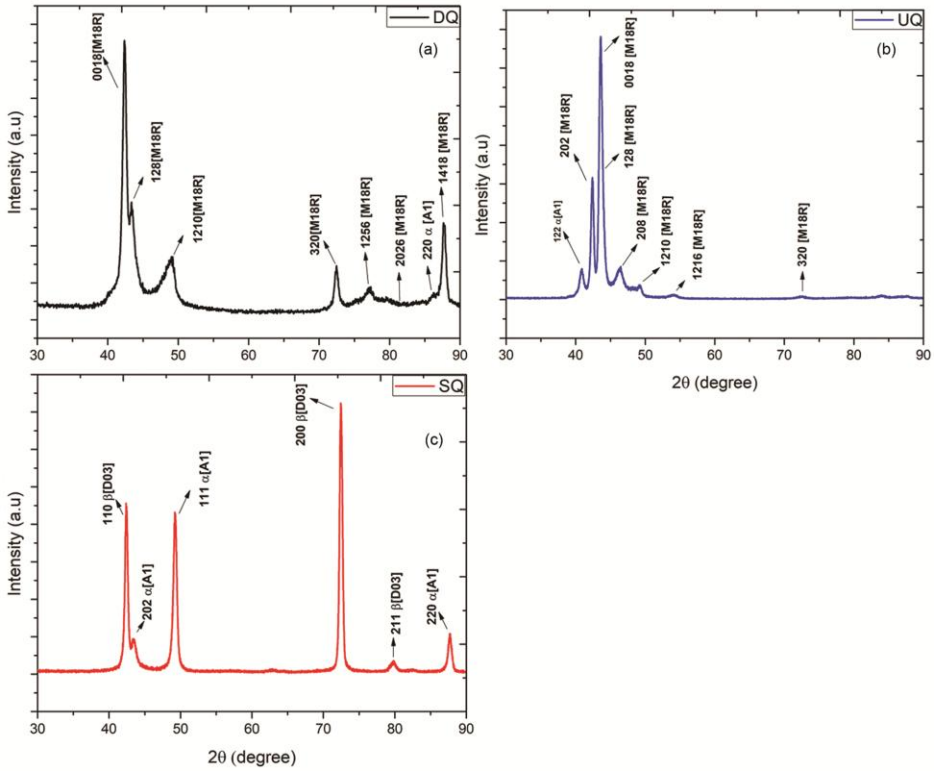

Fig. 5 — Comparison between the diffractograms of (a) DQ, (b) UQ and (c) SQ sample of the Cu-28Zn-3Al alloy. The peaks showing the existence of of α + β′ [M18R] in DQ, and UQ, whereas α + β [D03] in SQ condition.

Table 6 — Lattice parameters of the phases in the Cu-28Zn-3Al wt. % alloy after quenching with various methods

Quenching Method	Phase	Lattice Parameter	hkl
DQ	M18R	a = 4.427	0018
		b = 5.335	128
		c = 38.421	1210
		β = 88.35	2016
		φ = 0.93	320
			2026
			1418
	α[[A1]	a = 3.62	220
UQ	M18R	a = 4.429	0018
		b = 5.331	128
		c = 38.453	1210
		β = 88.56	2016
		φ = 0.98	1220
			320
			2026
	α[[A1]	a = 3.62	111
SQ	β [D03]	a = 5.88	110
			200
			211
	α[[A1]	a = 3.62	111
			220

and β [D03] phases marked by peaks (110) [A1] and (211) β [D03][6]. The SQ lattice parameter values in Table 5. shows that both phases in the SQ sample have a cubic crystal structure.

From the analysis, it can be concluded that the DQ and UQ quenching method produce β′ [M18R] martensite phase as the matrix with V-shape, similar to the study of Asanovic et al.[14] and the retained α [A1] as the second phase[10]. The volume fraction (β′ [M18R] : α) of DQ and UQ are [98.4:1.6] and [92.9:6.1], respectively. While SQ sample consists of 2 phases, that is α [A1] + β [D03] with the volume fraction of [51:49]. Phase transformation did not occur in the SQ sample because holding temperature of 100 ℃ is above the Ms temperature. So, the β [A2] phase cannot transform into martensite β′ [M18R], instead undergo ordering to form β [D03] phase. This result is in line with previous research by Stošić et al.[10] using the Cu-25Zn-4Al wt. % (α + β [D03]) and Cu-30Zn-4Al wt. % (β [D03]) alloys. The alloy with single-phase (Cu-30Zn-4Al wt. %) did not show any phase transformation. Whereas in the sample, Cu-25Zn-4Al wt. % (α + β [D03]) with the SQ method caused the formation of V form martensite and retained α. This confirms that the choice of composition and quenching method will affect the microstructure of SMA. The type of martensite depends on the e/a value. If e/a > 1.52, it will produce

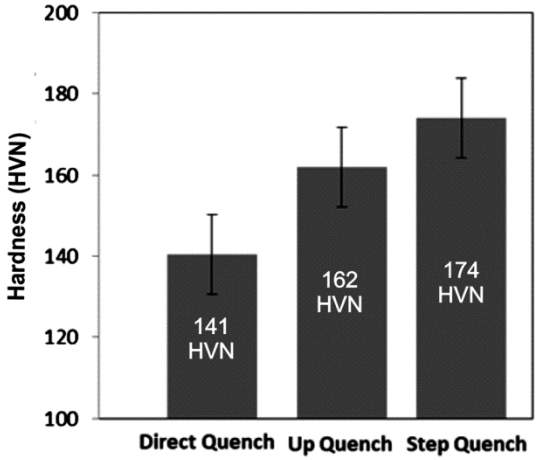

Fig. 6 — Microhardness of DQ, UQ and SQ samples of Cu-28Zn-3Al wt. %.

the 2H martensite phase, but if e/a is in the range of 1.4-1.48, it will produce the M18R or 9R martensite[8]. Martensite phase generally has V-shape or needle-like. The Cu-28Zn-3Al alloy has an e /a of 1.40, so that the martensite phase formed is M18R, and this was confirmed through XRD.

Figure 6 explicates the comparison of Vickers microhardness of the DQ, UQ, and SQ samples. The DQ had lower hardness than UQ and SQ, that might be due to higher entrapped vacancies as a result of direct quenching from 850 ℃ to ± 4 ℃, without further heating. On the contrary, the 100 ℃ heating treatment on UQ and SQ diffused the vacancies into grain boundary and then dissipated. In addition, the heating treatment on UQ sample rearranged the stacking sequence of the β' [M18R] martensite phase, which caused the formation of harder and more compact martensite.

From the analysis above, it can be concluded that DQ and UQ quenching method produced β' [M18R] martensite together with small and well distributed retained α [A1]. In contrast, the alloy with SQ cooling originated the duplex phase (α [A1] and β [D03]) and did not show the formation of the martensite phase.

3.3 Phase Transformation

Phase transformation of DQ, UQ and SQ samples was characterized by using a DSC instrument and the results are shown through curves of heat flow to temperature in Fig. 7. The peak of phase transformation is seen in the DQ and UQ samples, but is absent in the SQ. This indicates that the phase transformation only occurs in the DQ and UQ samples. The phase transformation temperature of each sample is summarized in Table 7.

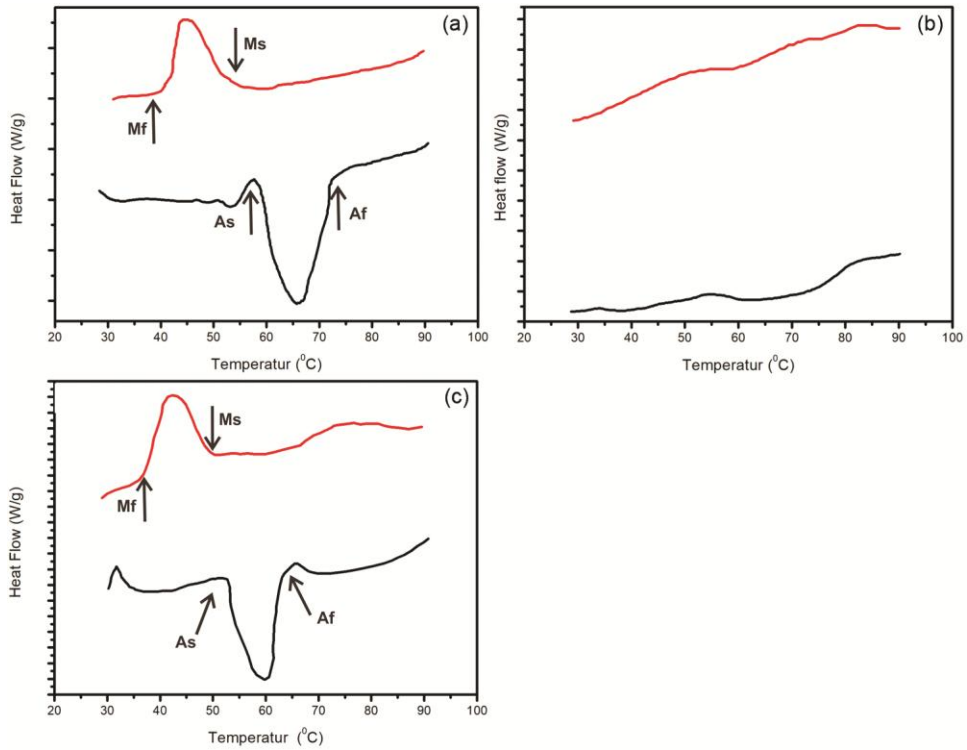

Fig. 7 — DSC thermogram for (a) DQ (b) UQ, and (c) SQ of Cu-28Zn-3Al wt. % alloy.

Table 7 — Transformation temperatures of Cu-28Zn-3Al wt. % with various quenching method

Sample	Transformation Temperature (°C)			
	M_s	M_f	A_s	A_f
DQ	52.4	38.3	59.7	71.6
UQ	50.1	38.1	53.3	63
SQ	-	-	-	-

Table 8 — Strain recovery of the Cu-28Zn-3Al wt. % with various quenching methods

Quenching Method	Strain Recovery
DQ	27.2%
UQ	36.3%
SQ	-

From Table 7 it can be seen that phase transformation temperatures (M_s, M_f, A_s and A_f) of the UQ sample is lower than those of the DQ sample, even though the difference is not significant. This is because of the 100 ℃ heating treatment in UQ that reduced vacancies and stabilized the martensite.

3.4 SME

The strain recovery of sample with various quenching method is shown in Table 8. It showed that the strain recovery of the UQ sample is higher than that of the DQ sample 36.3%, and 27.2%, respectively. The SQ samples did not show any recovery after bending tests due to the absence of martensite phase, so that no phase transformation occurred. It confirms the results of microstructure, XRD, EDS, and DSC observation.

Table 8 shows that the UQ strain recovery is higher because the phase in the UQ sample is more easily transforms, marked with smaller the hysteresis temperatures (T_h). This is due to the UQ treatment can eliminate vacancies which cause stable martensite. Gil et al.[15] mentioned that the vacancies formed due to quenching caused the interphase movement of the martensite plate to be obstructed, so that the SME decreased, and this was marked by an increase in T_h. Through the calculation, it is known that T_h of UQ is lower than T_h of DQ. T_h interprets the level of energy produced by the martensite interface to transform when the transformation is difficult, T_h will be high.

4 Conclusion

- The as-cast and as-homogenized microstructure consist of two phases, which are the β [D03] as the matrix and α [A1] as the second phase in the form of lath. The homogenization process at 850 ℃ for 2h caused the aspect ratio (L/t) of α [A1] increased from 6 to 11.25 without significant changes neither in the volume fraction nor the hardness.
- The DQ and UQ quenching methods caused the formation of martensite phase β' [M18R] with V-

shape as the matrix and retained α [A1] as the second phase in a uniform distribution. The volume ratios of β' [M18R]:α [A1] of the DQ and UQ are [98.4:1.6] and [93.1:6], respectively.

- The SQ quenching method did not produce martensite, instead formed α [A1] and β [D03] with a volume ratio of [49:51]
- The M_s, M_f, A_s, and A_f, transformation temperatures of the DQ are 52.4, 38.3, 59.7, 71.6 ℃ and UQ are 50.1, 38.1, 53.3, 63 ℃, respectively. The strain recoveries of the DQ and UQ samples are 27.2% and 36.3%, respectively. This indicates that UQ quenching method produced better SME properties.

Acknowledgments

This research was supported by PMDSU Research Grant from Kementerian Riset dan Teknologi/Badan Riset dan Inovasi Nasional Republik Indonesia with contract No: NKB-439/UN2.RST/HKP.05.00/2020.

References

1 Wayman C M , & Duerig T W, *An introduction to martensite and shape memory in engineering aspects of shape memory alloys*, edited by Duerig T W (Butterworth-Heinemann, UK), 1990, 3.
2 Alaneme K K , & Okotete, E A, *Eng Sci & Tech Int J*, 19 (2016) 1582.
3 Dasgupta R, Jain A K, Kumar P, Hussein S, & Pandey A, *J Mat Res Tech*, *3* (2014) 264.
4 Wu M H, *Cu-based shape memory alloys in engineering aspects of shape memory alloys*, (Butterworth-Heinemann Ltd, UK), 1990, 69.
5 Lohan M N, Suru MG, Pricop B, & Bujoreanu L G, *Int J Min Met Mater*, 21 (2014) 1109.
6 Eskil M , & Kayali N, *Mater Lett*, 60 (2006) 630.
7 Lobo P S, Almeida J, & Guerreiro L, *Procedia Eng*, 114 (2015) 776.
8 Cuniberti A, Romero R, & Condo A, *Mater Sci Eng A*, 325 (2002) 177.
9 Chen F, Tian B, Tong Y, & Zheng Y, *Int J Mod Phys B*, 23 (2009) 1931.
10 Stošić Z, Manasijevića D, Balanovića L, Grgurićb T H, Stamenkovića U, Premovićc M, Minićc D, Gorgievskia M, & Todorovićd R, *Mater Sci*, 20 (2017) 1425.
11 Liang S M, & Rainer S F, *Calphad*, 52 (2016) 21.
12 Smirnov S V, Myasnikova, M V, & Pugacheva N B, *Int J Damage Mech*, 25 (2016) 251.
13 Leu S S, & Hu C T, The aging effect on Cu-Zn-Al shape memory alloys with low contents of aluminium, *Metall Mater Trans A*, 22 (1991) 25.
14 Asanovic A, Delijic A, & Jaukovic N, *Scr Mater*, 58 (2008) 599.
15 Gil F J, & Guilemany J M, *Thermochim Acta*, 205 (1992) 75.